Electronic Supplementary Material (ESI) for Physical Chemistry Chemical Physics.

Excited State Dynamics of 2'-Deoxyisoguanosine and Isoguanosine in Aqueous Solutions

Naishka E. Caldero-Rodríguez and Carlos E. Crespo-Hernández*

Department of Chemistry, Case Western Reserve University, Cleveland, OH 44106

* Corresponding author; E-mail: carlos.crespo@case.edu; ORCID: 0000-0002-3594-0890

Electronic Supporting Information

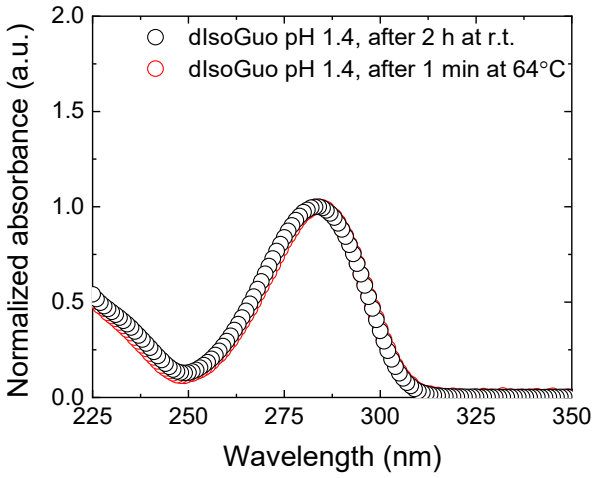

Figure S1. Normalized ground state absorption spectra of dIsoGuo in aqueous phosphate buffer solution at pH 1.4 measured after 2 hours of preparation (black) at room temperature (r.t.) and after heating for 1 minute at 64℃ and cooled down for 10 minutes (red).

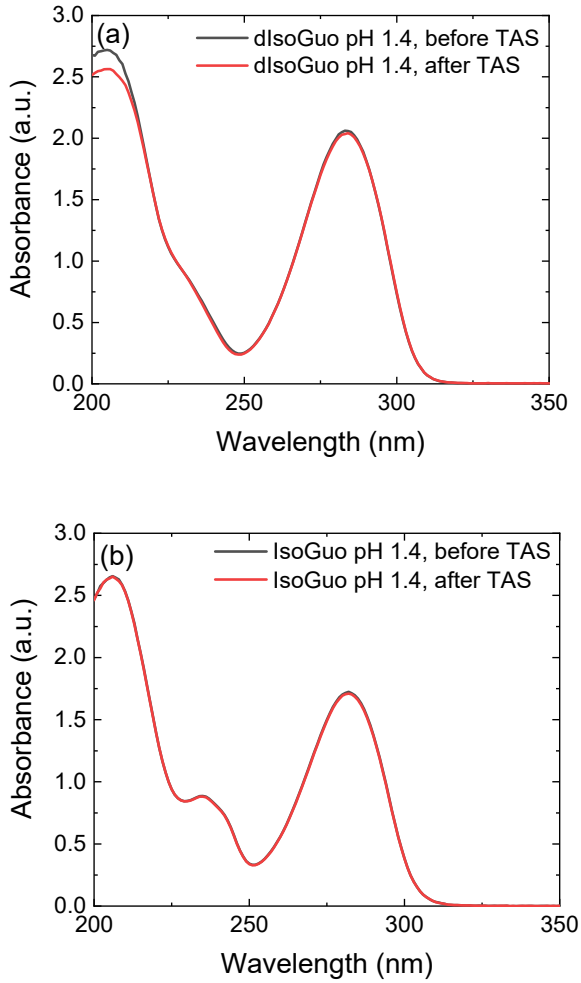

Figure S2. Ground state absorption spectra of (a) dIsoGuo and (b) IsoGuo in aqueous phosphate buffer solution at pH 1.4, before and after transient absorption spectroscopy measurements. Note that the change in absorbance at ca. 205 nm in Figure S2a is most likely due to instabilities on the absorbance signals due to the saturation of the detector in the spectrophotometer (not to photochemistry) as the absorbance of this band reaches an optical density larger than the linear dynamic range of the spectrometer.

Table S1. Optimized ground state energies corrected for the zero-point energy for neutral tautomers of dIsoGuo and IsoGuo, using DFT calculations in water at the B3LYP/IEFPCM/6-311++G(d,p) level of theory.

Neutral Tautomer	Δ E (eV)	Δ E (kcal mol^{-1})
***syn*-H1-IsoGuo**	**0**	**0**
syn-H3-IsoGuo	0.08	1.85
anti-H1-IsoGuo	0.16	3.77
anti-H3-IsoGuo	0.23	5.38
Neutral Tautomer	Δ E (eV)	Δ E (kcal mol^{-1})
***syn*-H1-dIsoGuo**	**0**	**0**
syn-H3-dIsoGuo	0.07	1.58
anti-H1-dIsoGuo	0.15	3.47
anti-H3-dIsoGuo	0.22	5.14

Table S2. Optimized ground state energies corrected for the zero-point energy for protonated tautomers of dIsoGuo and IsoGuo, using DFT calculations in water at the B3LYP/IEFPCM/6-311++G(d,p) level of theory.

Protonated Tautomer	Δ E (eV)	Δ E (kcal mol^{-1})
***syn*-H1,H3-IsoGuo**	**0**	**0**
anti-H1,H3-IsoGuo	0.22	5.05
syn-H1,H7-IsoGuo	0.39	8.89
anti-H1,H7-IsoGuo	0.43	9.95
syn-H3,H7-IsoGuo	0.43	10.01
anti-H3,H7-IsoGuo	0.58	13.30
Protonated Tautomer	Δ E (eV)	Δ E (kcal mol^{-1})
***syn*-H1,H3-dIsoGuo**	**0**	**0**
anti-H1,H3-dIsoGuo	0.22	5.18
syn-H1,H7-dIsoGuo	0.40	9.30
anti-H1,H7-dIsoGuo	0.43	9.80
syn-H3,H7-dIsoGuo	0.43	10.01
anti-H3,H7-dIsoGuo	0.57	13.11

Table S3. Vertical energies in eV for the relevant singlet and triplet transitions of the lowest energy tautomer of neutral IsoGuo (*syn*-H1-IsoGuo) in water obtained from TDDFT computations at the PBE0/IEFPCM/6-311++G(d,p)//B3LYP/IEFPCM/6-311++G(d,p) level of theory.

State	Transitions	% Contribution, Character	Primary Character	eV (oscillator)
S_1	H-0 → L+0	100.0, ππ*	ππ*(L_a)	4.3 (0.2039)
T_1	H-0 → L+0	100.0	ππ*	3.1
T_2	H-0 → L+1 H-0 → L+2	79.7 20.3	ππ*(ICT)	4.1

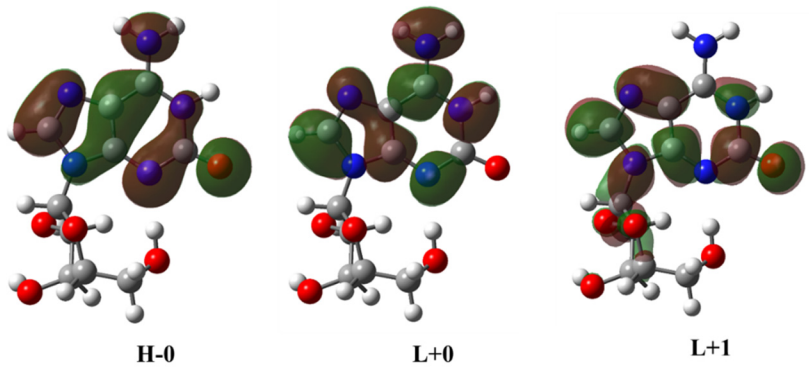

Scheme S1. Relevant Kohn-Sham orbitals for neutral IsoGuo (*syn*-H1-IsoGuo) in water obtained from TDDFT computations at the PBE0/IEFPCM/6-311++G(d,p)//B3LYP/IEFPCM/6-311++G(d,p) level of theory.

Table S4. Vertical energies in eV for the relevant singlet and triplet transitions of the lowest energy tautomer of neutral dIsoGuo (*syn*-H1-dIsoGuo) in water obtained from TDDFT computations at the PBE0/IEFPCM/6-311++G(d,p)//B3LYP/IEFPCM/6-311++G(d,p) level of theory.

State	Transitions	% Contribution, Character	Primary Character	eV (oscillator)
S_1	H-0 → L+0	100.0, ππ*	ππ*(L_a)	4.3 (0.2045)
T_1	H-0 → L+0	100.0	ππ*	3.1
T_2	H-0 → L+1 H-0 → L+2	92.5 7.5	ππ*(ICT)	4.1

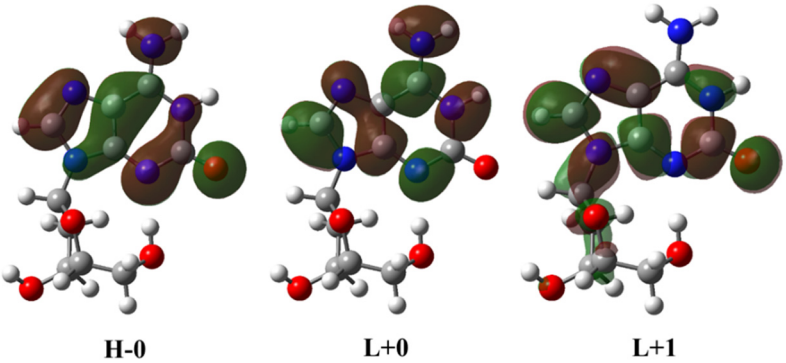

Scheme S2. Relevant Kohn-Sham orbitals for neutral dIsoGuo (*syn*-H1-dIsoGuo) in water obtained from TDDFT computations at the PBE0/IEFPCM/6-311++G(d,p)//B3LYP/IEFPCM/6-311++G(d,p) level of theory.

Table S5. Vertical energies in eV for the relevant singlet and triplet transitions of the lowest energy tautomer of protonated IsoGuo (*syn*-H1,H3-IsoGuo) in water obtained from TDDFT computations at the PBE0/IEFPCM/6-311++G(d,p)//B3LYP/IEFPCM/6-311++G(d,p) level of theory.

State	Transitions	% Contribution, Character	Primary Character	eV (oscillator)
S_1	H-0 → L+0	100.0, ππ*	ππ*(L_a)	4.6 (0.2317)
T_1	H-0 → L+0	100.0	ππ*	3.3
T_2	H-0 → L+1 H-0 → L+5	96.7 3.3	ππ*(ICT)	4.3

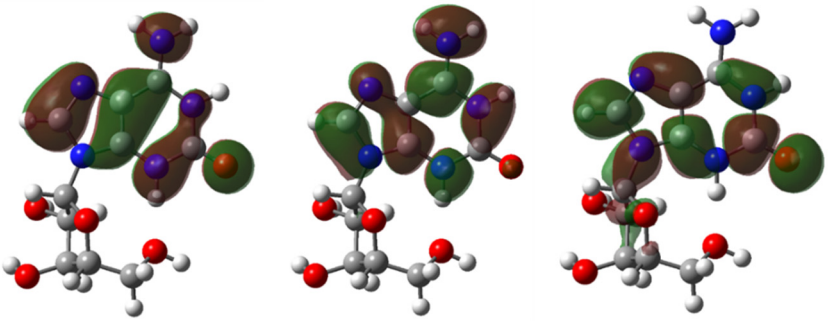

Scheme S3. Relevant Kohn-Sham orbitals for protonated IsoGuo (*syn*-H1,H3-IsoGuo) in water obtained from TDDFT computations at the PBE0/IEFPCM/6-311++G(d,p)//B3LYP/IEFPCM/6-311++G(d,p) level of theory.

Table S6. Vertical energies in eV for the relevant singlet and triplet transitions of the lowest energy tautomer of protonated dIsoGuo (*syn*-H1,H3-dIsoGuo) in water obtained from TDDFT computations at the PBE0/IEFPCM/6-311++G(d,p)//B3LYP/IEFPCM/6-311++G(d,p) level of theory.

State	Transitions	% Contribution, Character	Primary Character	eV (oscillator)
S_1	H-0 → L+0	100.0, ππ*	ππ*(L_a)	4.6 (0.2344)
T_1	H-0 → L+0	100.0	ππ*	3.3
T_2	H-9 → L+4 H-0 → L+1 H-0 → L+4	2.7 95.0 2.4	ππ*(ICT)	4.3

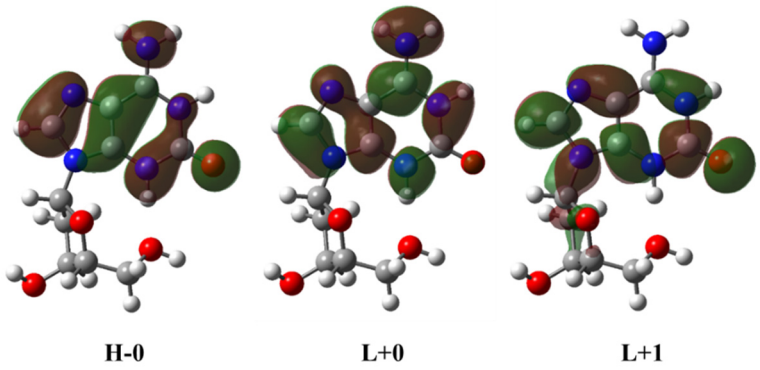

Scheme S4. Relevant Kohn-Sham orbitals for protonated dIsoGuo (*syn*-H1,H3-dIsoGuo) in water obtained from TDDFT computations at the PBE0/IEFPCM/6-311++G(d,p)//B3LYP/IEFPCM/6-311++G(d,p) level of theory.

Table S7. Optimized ground state energies for neutral tautomers of dIsoGuo and IsoGuo with microsolvation, using DFT calculations in water at the B3LYP/6-31+G(d,p) level of theory, followed by single-point energy calculations at the B3LYP/IEFPCM/6-311++G(d,p) level of theory.

Neutral Tautomer	Δ E (eV)	Δ E (kcal mol^{-1})
***syn*-H1-IsoGuo**	**0**	**0**
anti-H1-IsoGuo	0.09	2.07
syn-H3-IsoGuo	0.23	5.41
anti-H3-IsoGuo	0.40	9.33
Neutral Tautomer	Δ E (eV)	Δ E (kcal mol^{-1})
***syn*-H1-dIsoGuo**	**0**	**0**
anti-H1-dIsoGuo	0.14	3.30
syn-H3-dIsoGuo	0.21	4.80
anti-H3-dIsoGuo	0.37	8.61

Table S8. Optimized ground state energies for protonated tautomers of dIsoGuo and IsoGuo with microsolvation, using DFT calculations in water at the B3LYP/6-31+G(d,p) level of theory, followed by single-point energy calculations at the B3LYP/IEFPCM/6-311++G(d,p) level of theory.

Protonated Tautomer	Δ E (eV)	Δ E (kcal mol^{-1})
***syn*-H1,H3-IsoGuo**	**0**	**0**
anti-H1,H3-IsoGuo	0.20	4.55
syn-H1,H7-IsoGuo	0.28	6.46
anti-H1,H7-IsoGuo	0.35	8.12
syn-H3,H7-IsoGuo	0.42	9.64
anti-H3,H7-IsoGuo	0.56	12.81
Protonated Tautomer	Δ E (eV)	Δ E (kcal mol^{-1})
***syn*-H1,H3-dIsoGuo**	**0**	**0**
anti-H1,H3-dIsoGuo	0.30	6.83
syn-H1,H7-dIsoGuo	0.30	6.89
anti-H1,H7-dIsoGuo	0.42	9.67
syn-H3,H7-dIsoGuo	0.48	11.12
anti-H3,H7-dIsoGuo	0.63	14.64

Table S9. Vertical energies in eV for the relevant singlet and triplet transitions of the lowest energy tautomer of neutral IsoGuo (*syn*-H1-IsoGuo) with microsolvation, using TDDFT computations at the PBE0/IEFPCM/6-311++G(d,p)//B3LYP/6-31+G(d,p) level of theory.

State	Transitions	% Contribution, Character	Primary Character	eV (oscillator)
S_1	H-0 → L+0	100.0, ππ*	ππ*(L_a)	4.4 (0.2214)
T_1	H-0 → L+0	100.0	ππ*	3.2
T_2	H-0 → L+1 H-0 → L+2	97.4 2.6	ππ*(ICT)	4.1

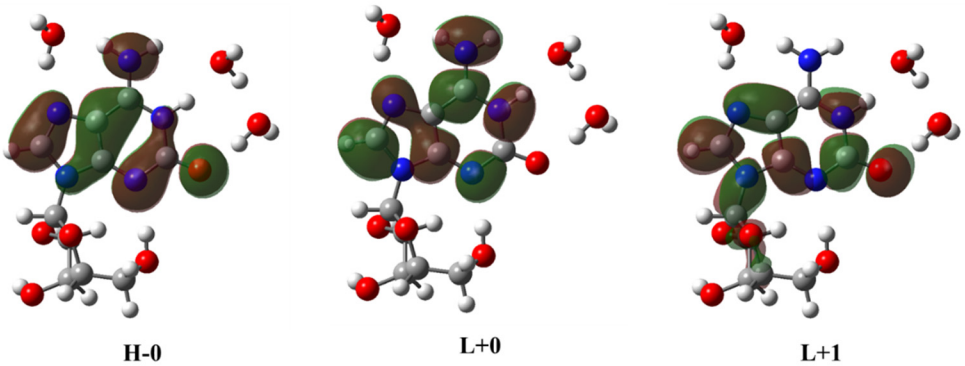

Scheme S5. Relevant Kohn-Sham orbitals for neutral IsoGuo (*syn*-H1-IsoGuo) with microsolvation, using TDDFT computations at the PBE0/IEFPCM/6-311++G(d,p)//B3LYP/6-31+G(d,p) level of theory.

Table S10. Vertical energies in eV for the relevant singlet and triplet transitions of the lowest energy tautomer of neutral dIsoGuo (*syn*-H1-dIsoGuo) with microsolvation, using TDDFT computations at the PBE0/IEFPCM/6-311++G(d,p)//B3LYP/6-31+G(d,p) level of theory.

State	Transitions	% Contribution, Character	Primary Character	eV (oscillator)
S_1	H-0 → L+0	100.0, ππ*	ππ*(L_a)	4.4 (0.2223)
T_1	H-0 → L+0	100.0	ππ*	3.2
T_2	H-0 → L+1 H-0 → L+2	97.5 2.5	ππ*(ICT)	4.1

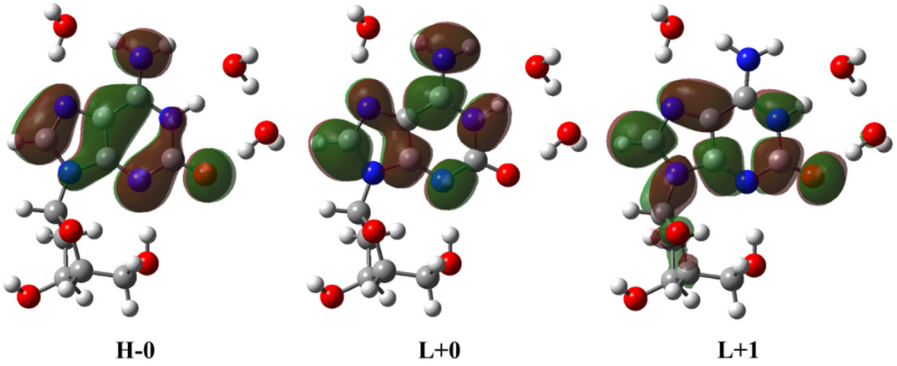

Scheme S6. Relevant Kohn-Sham orbitals for neutral dIsoGuo (*syn*-H1-dIsoGuo) with microsolvation, using TDDFT computations at the PBE0/IEFPCM/6-311++G(d,p)//B3LYP/6-31+G(d,p) level of theory.

Table S11. Vertical energies in eV for the relevant singlet and triplet transitions of the lowest energy tautomer of protonated IsoGuo (*syn*-H1,H3-IsoGuo) with microsolvation, using TDDFT computations at the PBE0/IEFPCM/6-311++G(d,p)//B3LYP/6-31+G(d,p) level of theory.

State	Transitions	% Contribution, Character	Primary Character	eV (oscillator)
S_1	H-0 → L+0	100.0, ππ*	ππ*(L_a)	4.7 (0.2514)
T_1	H-0 → L+0	100.0	ππ*	3.4
T_2	H-0 → L+1 H-0 → L+5	96.2 3.8	ππ*(ICT)	4.3

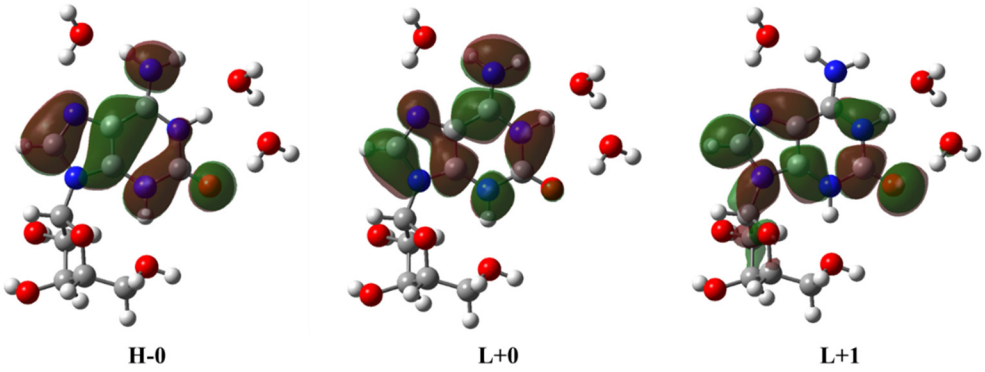

Scheme S7. Relevant Kohn-Sham orbitals for protonated IsoGuo (*syn*-H1,H3-IsoGuo) with microsolvation, using TDDFT computations at the PBE0/IEFPCM/6-311++G(d,p)//B3LYP/6-31+G(d,p) level of theory.

Table S12. Vertical energies in eV for the relevant singlet and triplet transitions of the lowest energy tautomer of protonated dIsoGuo (*syn*-H1,H3-dIsoGuo) with microsolvation, using TDDFT computations at the PBE0/IEFPCM/6-311++G(d,p)//B3LYP/6-31+G(d,p) level of theory.

State	Transitions	% Contribution, Character	Primary Character	eV (oscillator)
S_1	H-0 → L+0	100.0, ππ*	ππ*(L_a)	4.7 (0.2543)
T_1	H-0 → L+0	100.0	ππ*	3.4
T_2	H-12 → L+5 H-0 → L+1 H-0 → L+5	2.8 93.3 3.9	ππ*(ICT)	4.3

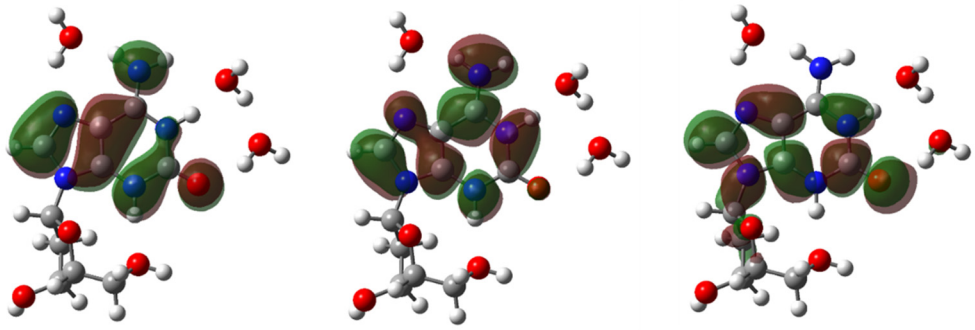

Scheme S8. Relevant Kohn-Sham orbitals for the lowest energy tautomer of protonated dIsoGuo (*syn*-H1,H3-dIsoGuo) with microsolvation, using TDDFT computations at the PBE0/IEFPCM/6-311++G(d,p)//B3LYP/6-31+G(d,p) level of theory.

Table S13. Vertical energies in eV for the relevant singlet and triplet transitions of protonated tautomer *anti*-H1,H3-dIsoGuo with microsolvation, using TDDFT computations at the PBE0/IEFPCM/6-311++G(d,p)//B3LYP/6-31+G(d,p) level of theory.

State	Transitions	% Contribution, Character	Primary Character	eV (oscillator)
S_1	H-0 → L+0	100.0, ππ*	ππ*(L_a)	4.7 (0.2824)
T_1	H-0 → L+0	100.0	ππ*	3.4
T_2	H-0 → L+1 H-0 → L+3 H-0 → L+4	93.3 2.8 4.0	ππ*(ICT)	4.3

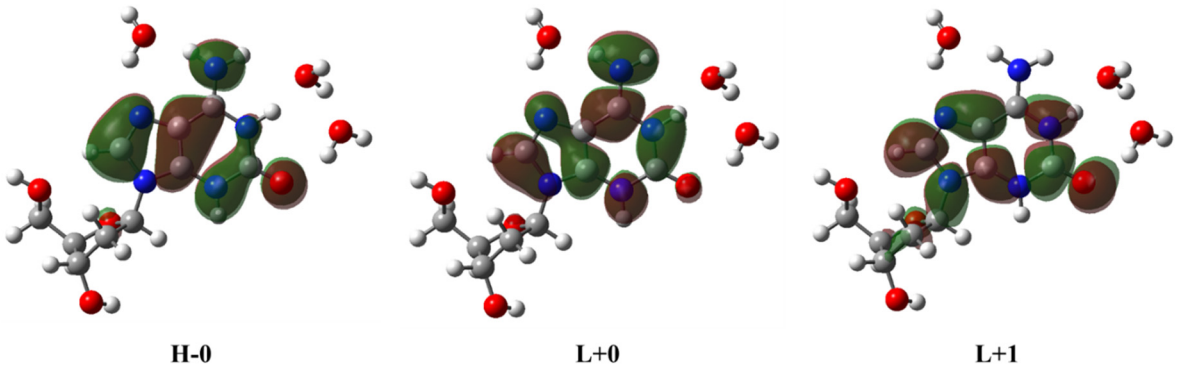

Scheme S9. Relevant Kohn-Sham orbitals for protonated tautomer *anti*-H1,H3-dIsoGuo with microsolvation, using TDDFT computations at the PBE0/IEFPCM/6-311++G(d,p)//B3LYP/6-31+G(d,p) level of theory.

Table S14. Vertical energies in eV for the relevant singlet and triplet transitions of the protonated *syn*-H3,H7-dIsoGuo with microsolvation, using TDDFT computations at the PBE0/IEFPCM/6-311++G(d,p)//B3LYP/6-31+G(d,p) level of theory.

State	Transitions	% Contribution, Character	Primary Character	eV (oscillator)
S_1	H-0 → L+0	100.0, ππ*	ππ*(L_a)	4.6 (0.2827)
T_1	H-0 → L+0	100.0	ππ*	3.3
T_2	H-1 → L+0 H-1 → L+1	84.3 15.7	ππ*(ICT)	4.0
T_3	H-0 → L+1 H-0 → L+5	97.7 2.3	ππ* (ICT)	4.4

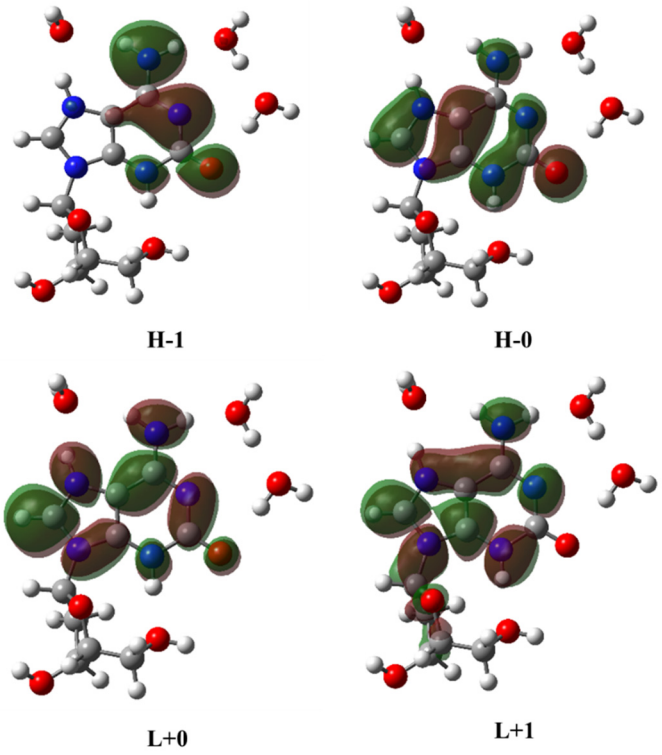

Scheme S10. Relevant Kohn-Sham orbitals for protonated tautomer *syn*-H3,H7-dIsoGuo with microsolvation, using TDDFT computations at the PBE0/IEFPCM/6-311++G(d,p)//B3LYP/6-31+G(d,p) level of theory.

Table S15. Vertical energies in eV for the relevant singlet and triplet transitions of the double-protonated tautomer *syn*-H1,H3,H7-dIsoGuo in water with microsolvation, using TDDFT computations at the PBE0/IEFPCM/6-311++G(d,p)//B3LYP/6-31+G(d,p) level of theory.

State	Transitions	% Contribution, Character	Primary Character	eV (oscillator)
S_1	H-0 → L+0	100.0, ππ*	ππ*(L_a)	4.6 (0.2690)
T_1	H-0 → L+0	100.0	ππ*	3.2
T_2	H-4 → L+0 H-0 → L+1	12.8 87.2	ππ*(ICT)	4.4
T_3	H-4 → L+0 H-4 → L+1 H-0 → L+1 H-0 → L+2	69.7 5.8 13.5 10.9	ππ*(ICT)	4.6

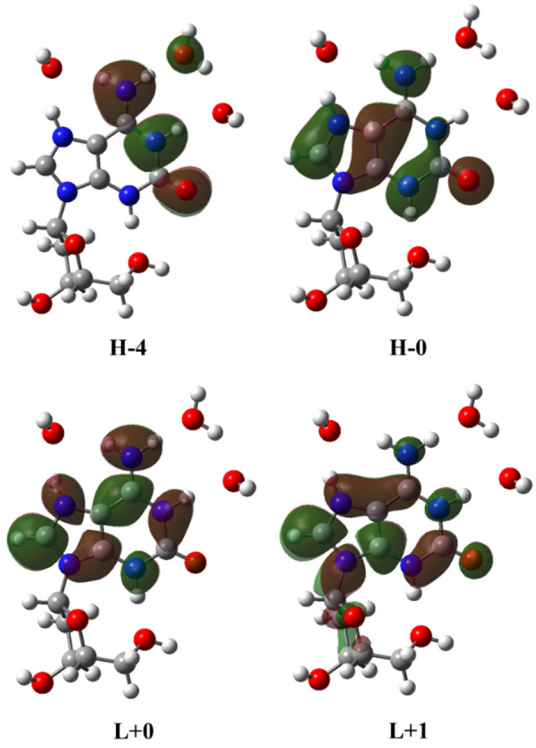

Scheme S11. Relevant Kohn-Sham orbitals for double-protonated tautomer *syn*-H1,H3,H7-dIsoGuo with microsolvation, using TDDFT computations at the PBE0/IEFPCM/6-311++G(d,p)//B3LYP/6-31+G(d,p) level of theory.

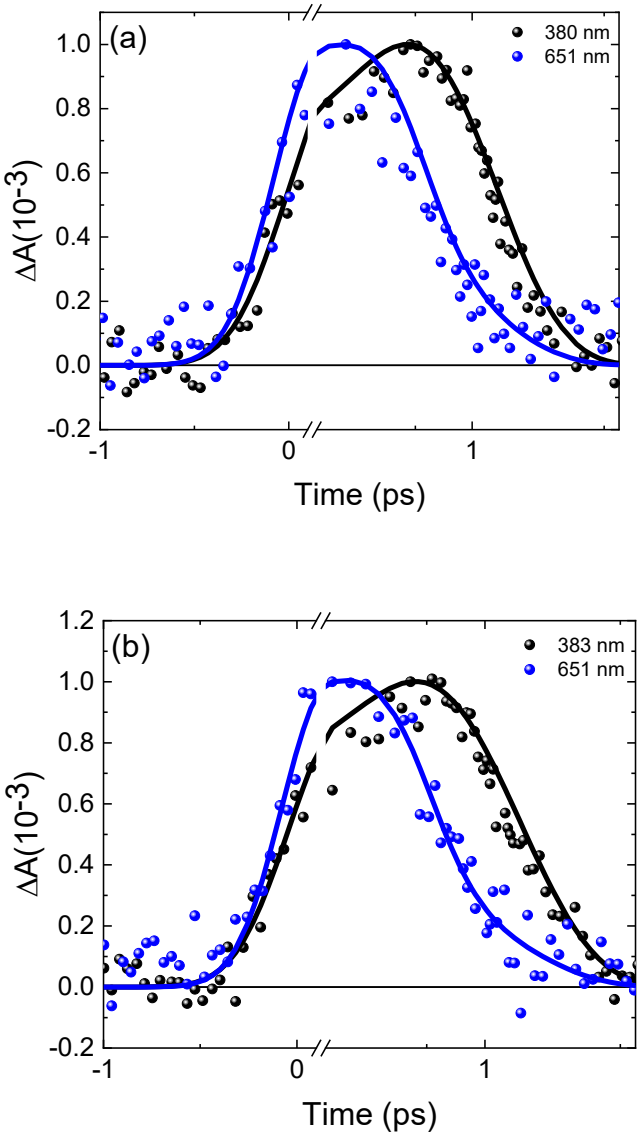

Figure S3. Normalized kinetic decay traces at the maximum amplitude of ΔA for (a) dIsoGuo and (b) IsoGuo in aqueous phosphate buffer solution at pH 7.4. Note that the x-axis is linear until 0.1 ps, after which a log scale is used.

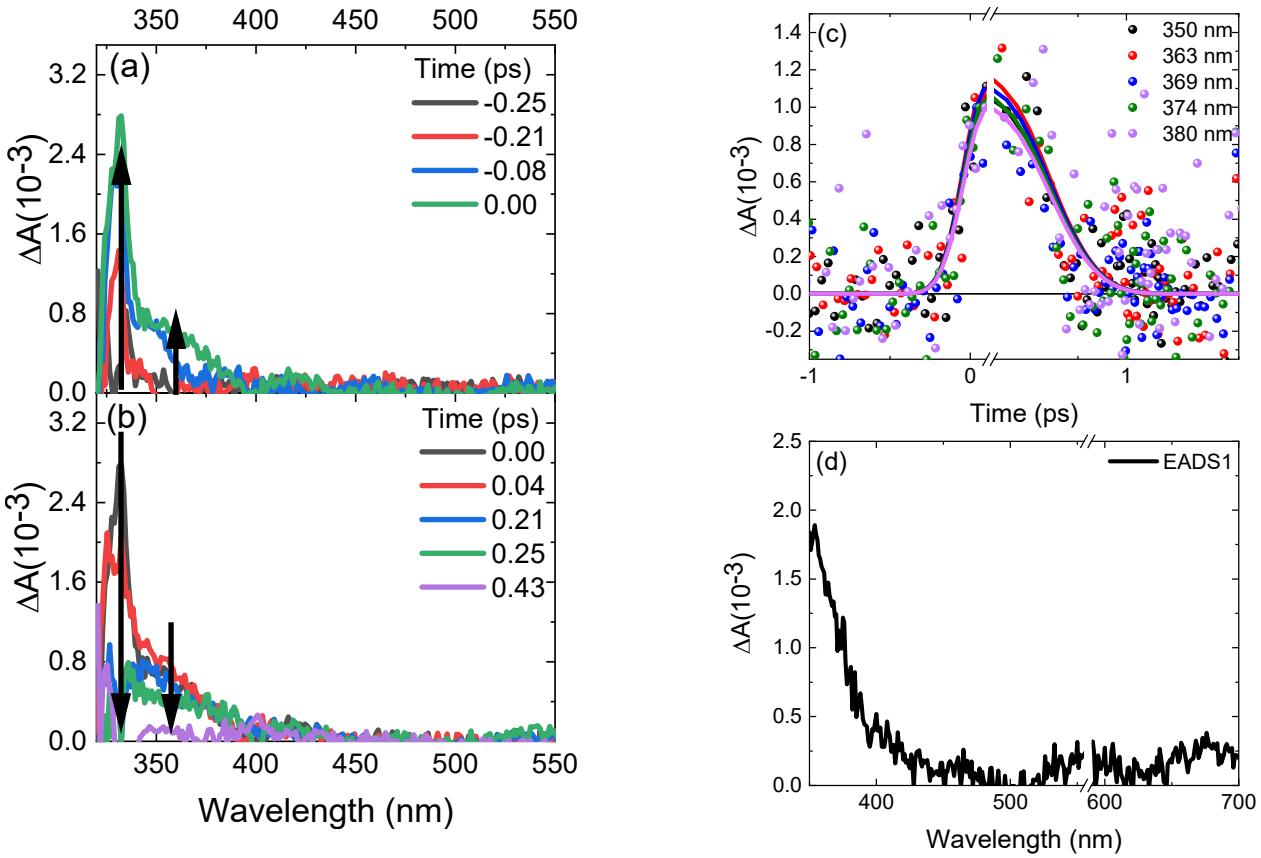

Figure S4. (a and b) The transient absorption spectra of solvent-only signal in aqueous phosphate buffer solution at pH 7.4, following 286 nm excitation. Time zero was determined at the maximum amplitude of ΔA, within the cross correlation of the pump and probe beams showed in panel a. (c) Representative kinetic decay traces are presented, featuring global analysis using a one-component exponential kinetic model. Note that the x-axis of panel c is linear until 0.1 ps, after which a log scale is used. (d) Evolution associated difference spectra (EADS) is presented, corresponding to the 350 to 700 nm region. Notice that there is also a break in the x-axis of panel d to conceal the overtone of the pump beam.

Table S16. Lifetime obtained for the solvent-only coherence signal in the aqueous solutions.

	τ_1 (ps)
pH 7.4	0.207 ± 0.009
pH 1.4	0.05 ± 0.07

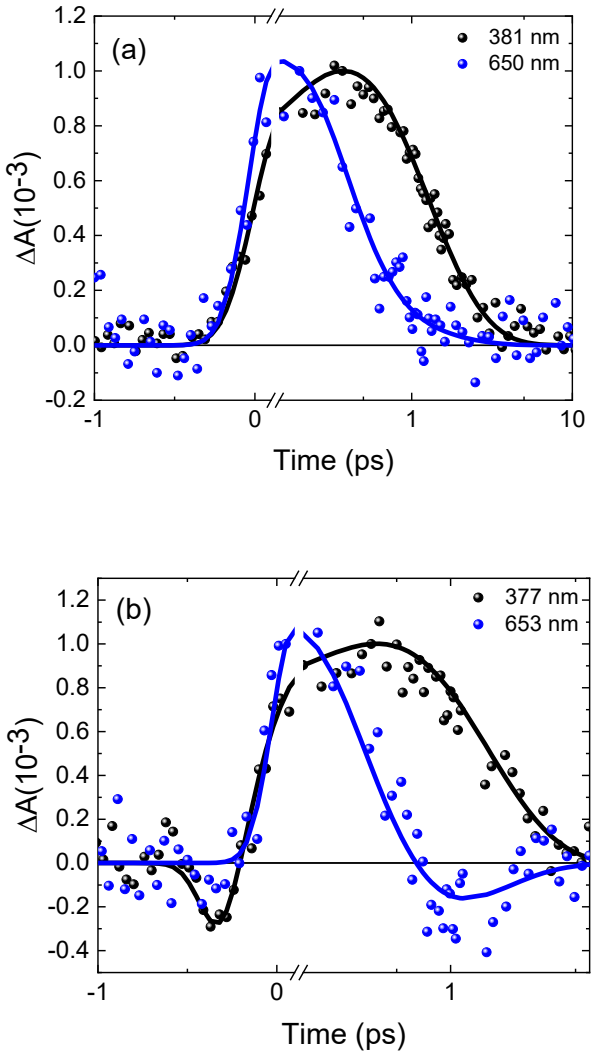

Figure S5. Normalized kinetic decay traces at the maximum amplitude of ΔA for (a) dIsoGuo and (b) IsoGuo in aqueous phosphate buffer solution at pH 1.4. Note that the x-axis is linear until 0.1 ps, after which a log scale is used. The negative "signal" predicted by the Glotaran program around 1 ps is believed to be an artifact due to the relatively poor signal-to-noise of the raw data.

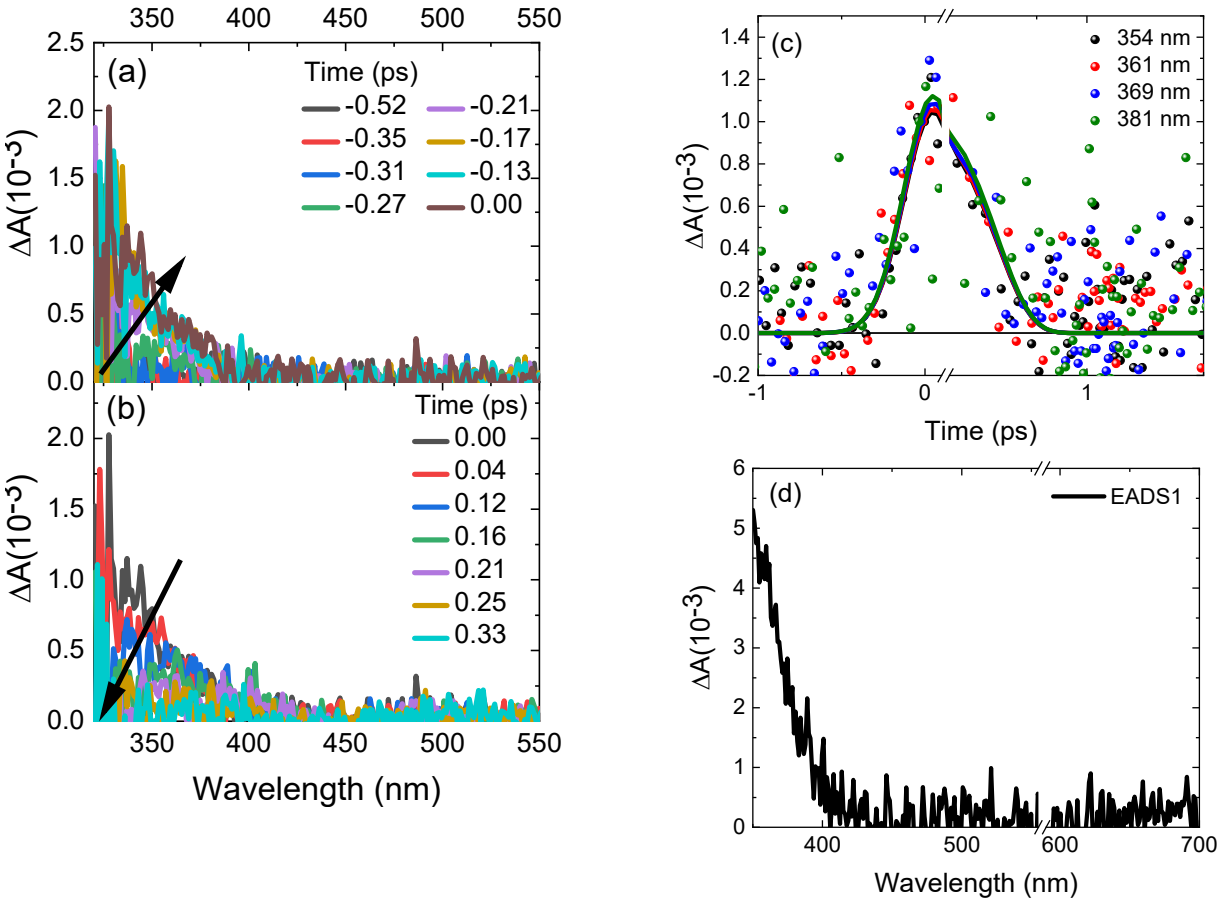

Figure S6. (a and b) The transient absorption spectra of solvent-only coherent signal in aqueous phosphate buffer solution at pH 1.4, following 286 nm excitation. Time zero was determined at the maximum amplitude of absorption, within the cross correlation of the pump and probe beams showed in panel a. (c) Representative kinetic decay traces are presented, featuring global analysis using a one-component exponential kinetic model. Note that the x-axis of panel c is linear until 0.1 ps, after which a log scale is used. (d) Evolution associated difference spectra (EADS) is presented, corresponding to the 350 to 700 nm region. Notice that there is also a break in the x-axis of panel d to remove the overtone of the pump beam.

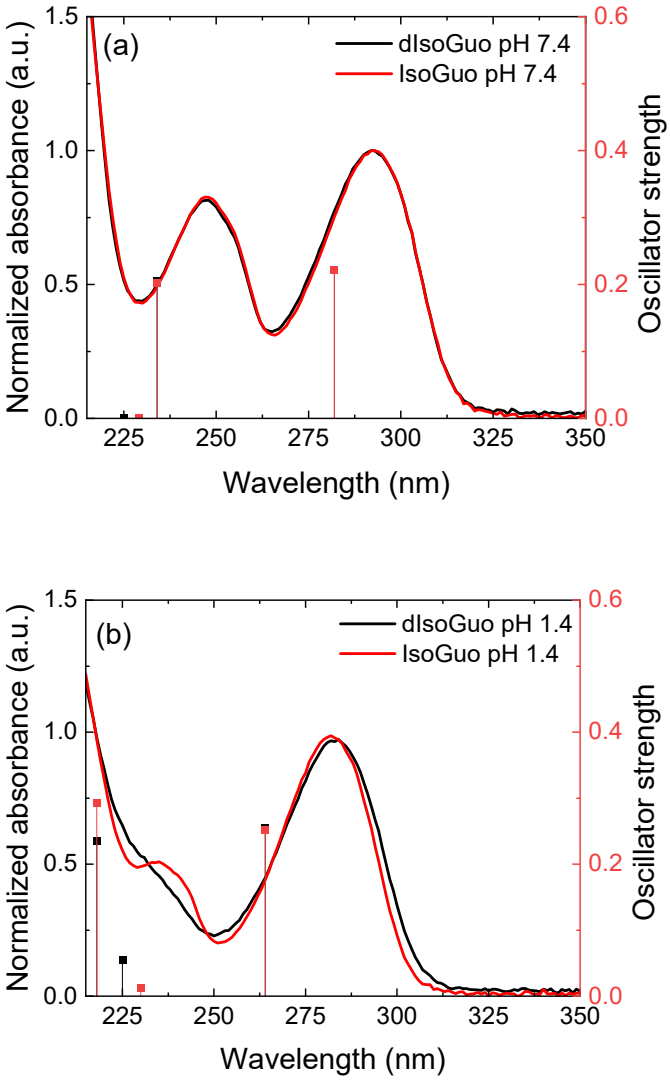

Figure S7. Normalized ground state absorption spectra of dIsoGuo (black) and IsoGuo (red) in aqueous phosphate buffer solution at (a) pH 7.4 and (b) pH 1.4, together with vertical excitation energies (VEE, nm) and oscillator strengths for the lowest energy tautomer of each molecule (*syn*-H1-dIsoGuo and *syn*-H1-IsoGuo for the neutral species, and *syn*-H1,H3-dIsoGuo and *syn*-H1,H3-IsoGuo for the protonated species) with microsolvation. TDDFT computations in water were performed at the PBE0/IEFPCM/6-311++G(d,p)//B3LYP/6-31+G(d,p) level of theory.

.

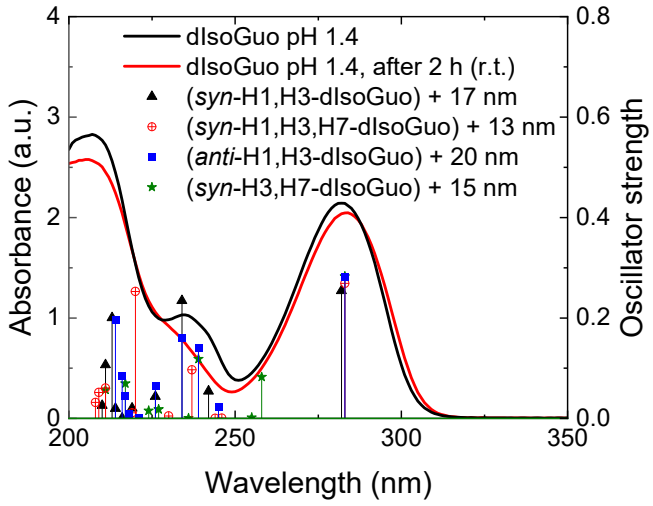

Figure S8. Ground state absorption spectra of dIsoGuo in aqueous phosphate buffer solution at pH 1.4 measured through time at room temperature (r.t.), with calculated vertical excitation energies (VEE, nm) and oscillator strengths for the protonated tautomers *syn*-H1,H3-dIsoGuo, *anti*-H1,H3-dIsoGuo, *syn*-H3,H7-dIsoGuo, and double-protonated tautomer *syn*-H1,H3,H7-dIsoGuo with microsolvation. TDDFT computations in water were performed at the PBE0/IEFPCM/6-311++G(d,p)//B3LYP/6-31+G(d,p) level of theory. Vertical excitation energies have been redshifted by a few nanometers to match the maximum of the lowest energy absorption band.

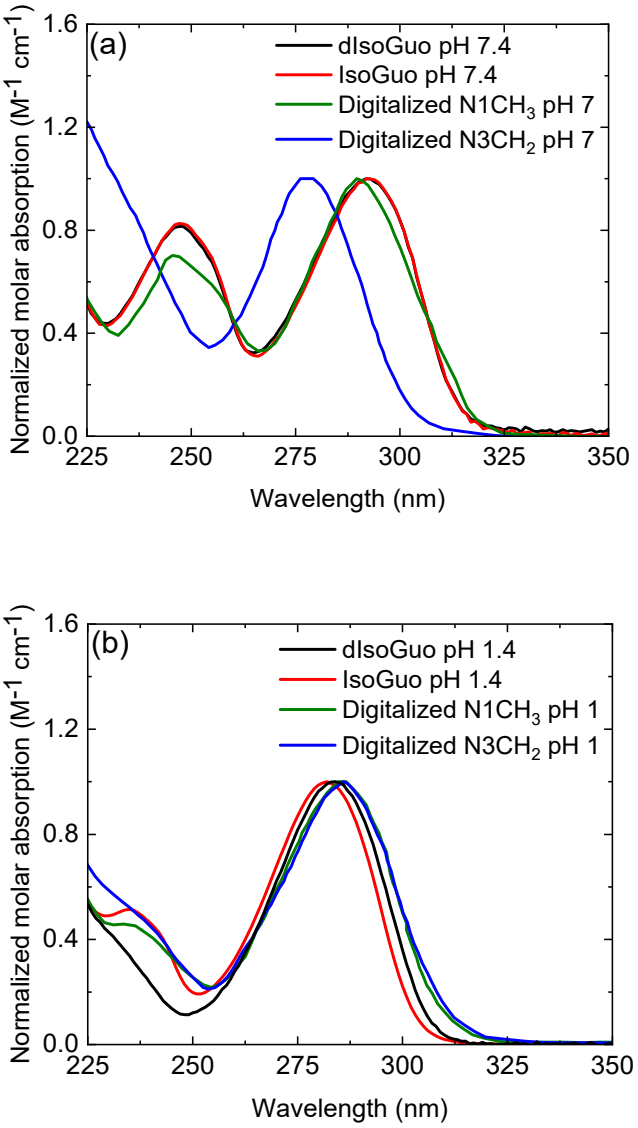

Figure S9. Normalized molar absorption spectra of dIsoGuo (black) and IsoGuo (red) in aqueous phosphate buffer solution at (a) pH 7.4 and (b) pH 1.4, with the digitalized molar absorption spectra of 2'-deoxy-1-methylisoguanosine (H1 fixed tautomer, $N1CH_3$, green) and the N3-isoguanine nucleoside derivative (H3 fixed tautomer, $N3CH_2$, blue) in water at the corresponding pH.[1]

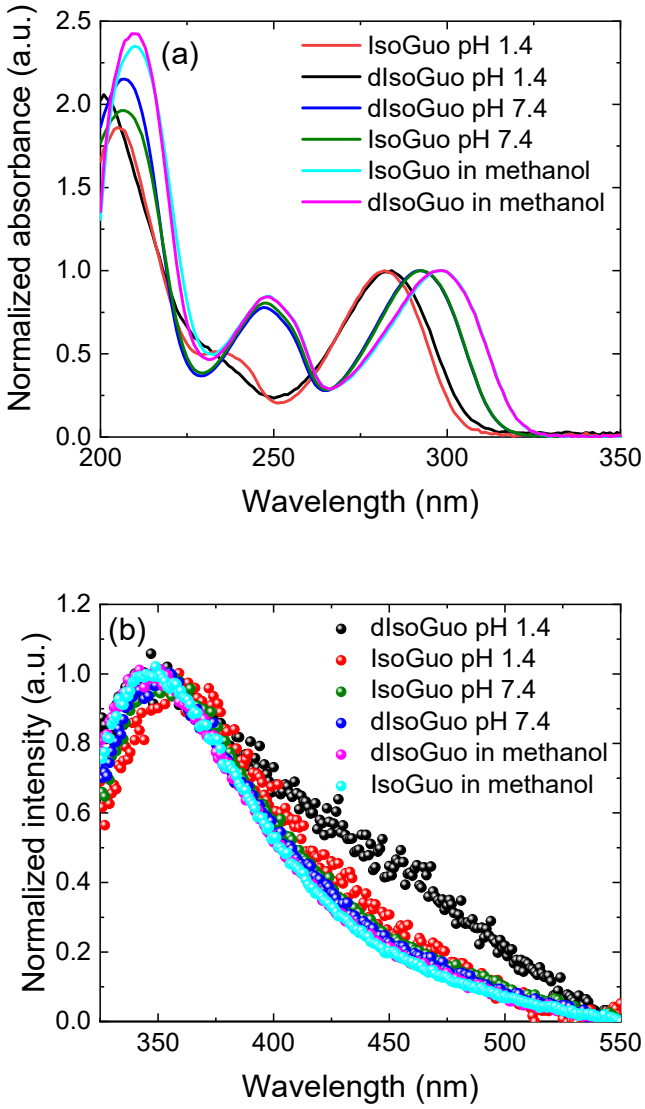

Figure S10. Normalized ground state absorption spectra of dIsoGuo and IsoGuo in aqueous phosphate buffer solution at pH 7.4 (blue and green, respectively) and pH 1.4 (black and red, respectively) and methanol (magenta and cyan, respectively). (b) Normalized ground state emission spectra of dIsoGuo and IsoGuo in aqueous phosphate buffer solution at pH 7.4 and pH 1.4 and methanol were also included. The emission spectrum of dIsoGuo in aqueous phosphate buffer solution at pH 1.4 was recorded after heating the sample at 64°C. Emission spectra were obtained using an excitation wavelength of 285 nm and were recorded at 800 V, keeping both the excitation and emission slit at 5 nm, with a scan rate of 120 nm/min.

Kwok and coworkers studied the excited state dynamics of 2'-deoxyguanosine (dG) and 2'-deoxyguanosine 5'-monophosphate (dGMP) in water and methanol.[2] Transient absorption measurements obtained upon excitation at 285 nm showed evidence of two main relaxation pathways. These nonradiative mechanisms contain the decay through a channel involving the lowest excited $^1\pi\pi^*(L_a)$ state and a decay through a weakly emissive state they assigned to a $^1\pi\sigma^*$ state. It was observed that the participation of the latter state is greater in methanol than water. These observations are present in the fluorescence spectra of dG, where the change from water to methanol causes the presence of a second emission band in the spectrum around 520 nm, which was assigned to this $^1\pi\sigma^*$ state. Krul and coworkers also supported the involvement of a $^1\pi\sigma^*$ state in the excited state dynamics of 7-deazaguanosine and guanosine 5'-monophosphate.[3] However, Figure S10b does not show the involvement of a $^1\pi\sigma^*$ state in the excited state dynamics of dIsoGuo and IsoGuo in aqueous phosphate buffer solutions since no additional emission bands are observed when using methanol as the solvent.

Supporting References

1. F. Seela, C. Wei and Z. Kazimierczuk, *Helv. Chim. Acta*, 1995, **78**, 1843-1854.
2. C. C.-W. Cheng, C. Ma, C. T.-L. Chan, K. Y.-F. Ho and W.-M. Kwok, *Photochem. Photobiol. Sci.*, 2013, **12**, 1351-1365.
3. S. E. Krul, S. J. Hoehn, K. Feierabend and C. E. Crespo-Hernández, *J. Chem. Phys.*, 2021, **154**, 075103-075113.